CNRS
Centre National de la Recherche Scientifique

INFN
Istituto Nazionale di Fisica Nucleare

Upper limits and constraints on stochastic backgrounds with non-standard polarizations

G. Cella, F. Di Renzo

Code: VIR-0456A-13
Issue: 0
Date : October 16, 2013

EGO, European Gravitational Observatory
Via E. Amaldi - 56021 Santo Stefano a Macerata-Cascina-Pisa-Italy
Telephone +39.050.752521 - Fax +39.050.752550

Abstract

Lorem ipsum dolor sit amet, consectetuer adipiscing elit. Etiam lobortis facilisis sem. Nullam nec mi et neque pharetra sollicitudin. Praesent imperdiet mi nec ante. Donec ullamcorper, felis non sodales commodo, lectus velit ultrices augue, a dignissim nibh lectus placerat pede. Vivamus nunc nunc, molestie ut, ultricies vel, semper in, velit. Ut porttitor. Praesent in sapien. Lorem ipsum dolor sit amet, consectetuer adipiscing elit. Duis fringilla tristique neque. Sed interdum libero ut metus. Pellentesque placerat. Nam rutrum augue a leo. Morbi sed elit sit amet ante lobortis sollicitudin. Praesent blandit blandit mauris. Praesent lectus tellus, aliquet aliquam, luctus a, egestas a, turpis. Mauris lacinia lorem sit amet ipsum. Nunc quis urna dictum turpis accumsan semper.

Contents

1 Introduction **1**
1.1 Overview of current results 3
1.2 Advanced detectors 4

2 Cross-correlation analysis: a brief overview **6**
2.1 Cross-correlation including non-standard polarizations 6
2.2 SNR for different polarizations 10
2.3 Detection, statistical considerations: sensitivity level 12

3 Prospects on future results **13**
3.1 SGWB sensitivity level 13
3.2 Frequency contribution to the SNR 17
3.3 Modes separation 17

4 Conclusions **19**

1 Introduction

The search for a stochastic background of gravitational waves (SGWB) is of fundamental importance in early universe cosmology and correspondingly in high energy physics. A successful detection or, less ambitiously, an upper limit constraint, could be of great interest in testing models for fundamental interactions.

One important field of investigation, related with the direct gravitational waves observation, is that of Extended Gravitational Theories (EGT), namely theories of gravity different than general relativity.

There are several motivations for looking at EGTs, namely

- they are important in order to test general relativity: it is useful to consider some alternative theories of gravity and see precisely how their physical predictions differ from those of general relativity;

- effective actions describing the low energy limit of models for the unification of fundamental interactions (like superstrings, supregravity, GUTs) tipically contains corrections terms to general relativity in the gravitational sector;
- they could be a step toward the solution for the gravity quantization problem: since the efforts in unifying quantum field theory with GR have not been fully successful, it is important to look for other classical theories of gravity to be quantized.

For these reasons it is important to keep on verifying GR experimentally to higher and higher degrees of accuracy, investigating or, at least, constraining alternative models.

Most viable theories of gravity are described by a symmetric rank-$(0,2)$ tensor, the metric, which completely determines the interaction of gravity with massive bodies. The differences between the theories lie in how the metric is affected by the presence of matter, in other words, the dynamics of the spacetime geometry itself. Most of these theories, including general relativity, incorporate local Lorentz invariance as well as being based upon second order differential equations. Since the wave operator (the D'Alambertian) is the Lorentz invariant 2nd order differential operator, it should be reasonable to suppose that most gravitational theories admit wave-like solutions [Will, 1993, §10.2].

GWs predicted by different theories could differ through:

- the propagation speed (e.g. in case of massive gravitons or extra-dimensions);
- the waveform, for any given source (cosmological or astrophysical it is);
- the polarization modes.

Here we limit ourselves by considering only differences in polarization modes predicted by the several viable theories. In particular, we will consider only weak, plane, nearly null gravitational waves in 4-dimensional spacetime, as defined in [Will, 1993, §10.2].

It can be shown that any general metric theory of gravity, with additional fields, degrees of freedom, or extra dimensions (once projected on our 3-space) can allow, at most, six polarization modes of a GW [Eardley et al., 1973]. For waves propagating in the z direction, the bases of the six polarizations can be defined as:

$$
\begin{aligned}
e^{+}_{ij} &= \begin{pmatrix} 1 & 0 & 0 \\ 0 & -1 & 0 \\ 0 & 0 & 0 \end{pmatrix} & e^{\times}_{ij} &= \begin{pmatrix} 0 & 1 & 0 \\ 1 & 0 & 0 \\ 0 & 0 & 0 \end{pmatrix} & e^{b}_{ij} &= \begin{pmatrix} 1 & 0 & 0 \\ 0 & 1 & 0 \\ 0 & 0 & 0 \end{pmatrix} \\
e^{x}_{ij} &= \begin{pmatrix} 0 & 0 & 1 \\ 0 & 0 & 0 \\ 1 & 0 & 0 \end{pmatrix} & e^{y}_{ij} &= \begin{pmatrix} 0 & 0 & 0 \\ 0 & 0 & 1 \\ 0 & 1 & 0 \end{pmatrix} & e^{\ell}_{ij} &= \sqrt{2} \begin{pmatrix} 0 & 0 & 0 \\ 0 & 0 & 0 \\ 0 & 0 & 1 \end{pmatrix}
\end{aligned} \tag{1}
$$

Theoretical Model	e^+_{ij}	$e^\times_{ij}$	e^b_{ij}	e^ℓ_{ij}	e^x_{ij}	e^y_{ij}
Einstein's General Relativity (GR)	*	*				
GR in a noncompactified 5D Minkowski sp.	*	*	†	†	*	*
GR in a noncompactified 6D Minkowski sp.	*	*	*	*	*	*
5D Kaluza-Klein theory	*	*	*		*	*
Randall-Sundrum braneworld	*	*				
DGP braneworld (normal branch)	*	*				
DGP braneworld (self-accelerating branch)	*	*	◊	△		
Brans-Dicke theory	*	*	◊	△		
$f(R)$ theory	*	*	◊	△		
Bimetric theory	*	*	◊	△	*	*

Table 1: GW polarization modes for various viable theories. Table taken from [Nishizawa et al., 2009, TABLE 1]. Modes † are correlated and behave as a single degree of freedom. If $m_g = 0$ then the △-modes vanishes; if $m_g \neq 0$ then the △- and ◊-modes are correlated.

The effect of each mode on a ring of test masses is represented in Figure 1. This will have a direct impact on the way in which a given gravitational wave will couple to a detector, as we will see.

Each polarization mode can be classified using its rotational symmetry around the GW propagation axis. Looking at the definitions (1) we see that e^b_{ij} and e^ℓ_{ij} behave as scalars, e^x_{ij} and e^y_{ij} as the two components of a (bidimensional) vector and e^+_{ij}, $e^\times_{ij}$ as the two components of a (bidimensional) symmetric and traceless tensor. This property does not depend, of course, on the specific theory under consideration; the presence of, or a constraint about a certain mode can then be used to test a theory by means only of its symmetry properties. In other words, the observation of GWs polarization modes can be used as a powerful tool to probe or to constrain alternative theories of gravity in a model-independent way.

1.1 Overview of current results

No direct detection of GWs has yet been possible but many bounds and upper limits have been evaluated.

In B. P. Abbott et al. [2009] an upper limit on the energy density of the SGWB has been given, using LIGO S5 run data. Assuming a flat spectrum for Ω_{gw} it is $\Omega_{\rm gw}(f) < 6.9 \times 10^{-6}$ in the frequency band around 100 Hz, at 95% confidence. This result is represented in Figure 2: as can be seen, the upper limit is below the one provided by the nucleosynthesis bound.

A detailed study of the detectability of additional polarization modes has been given by Nishizawa et al. [2009], including the expected upper limits obtainable with advanced detectors (as foreseen in 2009).

Here we're going to provide some estimates using the projected advanced LIGO and advanced VIRGO sensitivities shown in Figure 3.

Currently, there are only few constraints available on the additional polarization modes of GWs. For the scalar mode, they came from [Nishizawa et al., 2009]

- the study of the orbital-period derivative for the binary pulsar $PSR\ B1913+16$. Observations agree with general relativity predictions at a conservative level of 1% error. Hence,

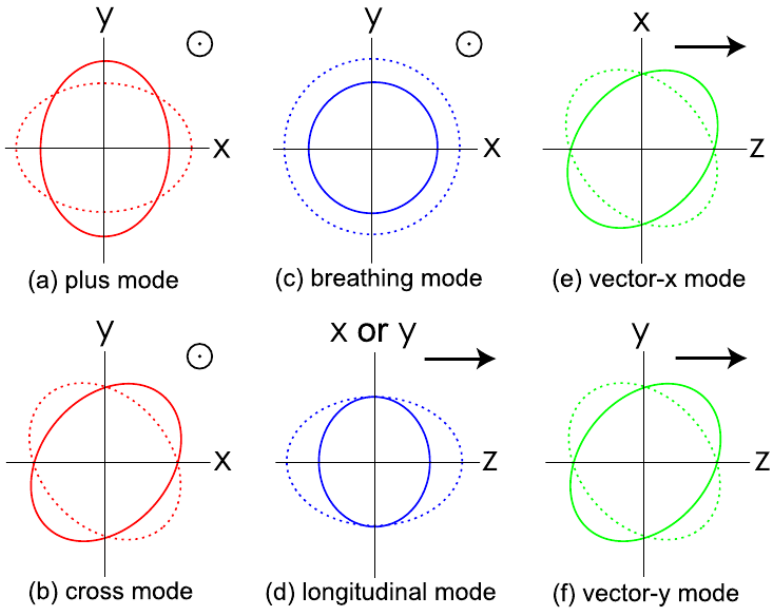

Figure 1: Graphical representation of how each polarization affects test masses arranged on a circle. Picture adapted from Nishizawa et al. [2009, FIG.1].

scalar GWs can contribute for less than 1% to the energy loss of the binary system;

- the measurements of the amplitude of scalar perturbations in the CMB at large angular scales (as observed in the WMAP data). These constrain the possible red shift of CMB photons due to the SGWB, and therefore limit the amplitude of the SGWB at largest wavelengths (smallest frequencies): $h_0^2\Omega_{\rm gw}^S \lesssim 10^{-12}$, over the range $10^{-18} \div 10^{-16}$ Hz.

With the new generation of advanced detectors a new observing scenario will open.

1.2 Advanced detectors

Over the next decade, several improvements have been scheduled for the next generation GW interferometric detectors Advanced LIGO (AdvLIGO) and Advanced Virgo (AdV) [Aasi, 2013]. These detectors are expected to yield the first direct observation of gravitational waves.

Hopefully, the GW experiments will be soon a key observational tool to obtain valuable informations about astronomical objects and physics of the early Universe.

The present discussion is meant to be an "update", for the article by Nishizawa et al., on non-standard polarization detectability, considering the improvements currently scheduled for the advanced interferometric detectors AdvLIGO and AdVirgo. Looking at Figure 3 we see that a final sensitivity improvement of about an order of magnitude is espected in the most relevant frequency band.

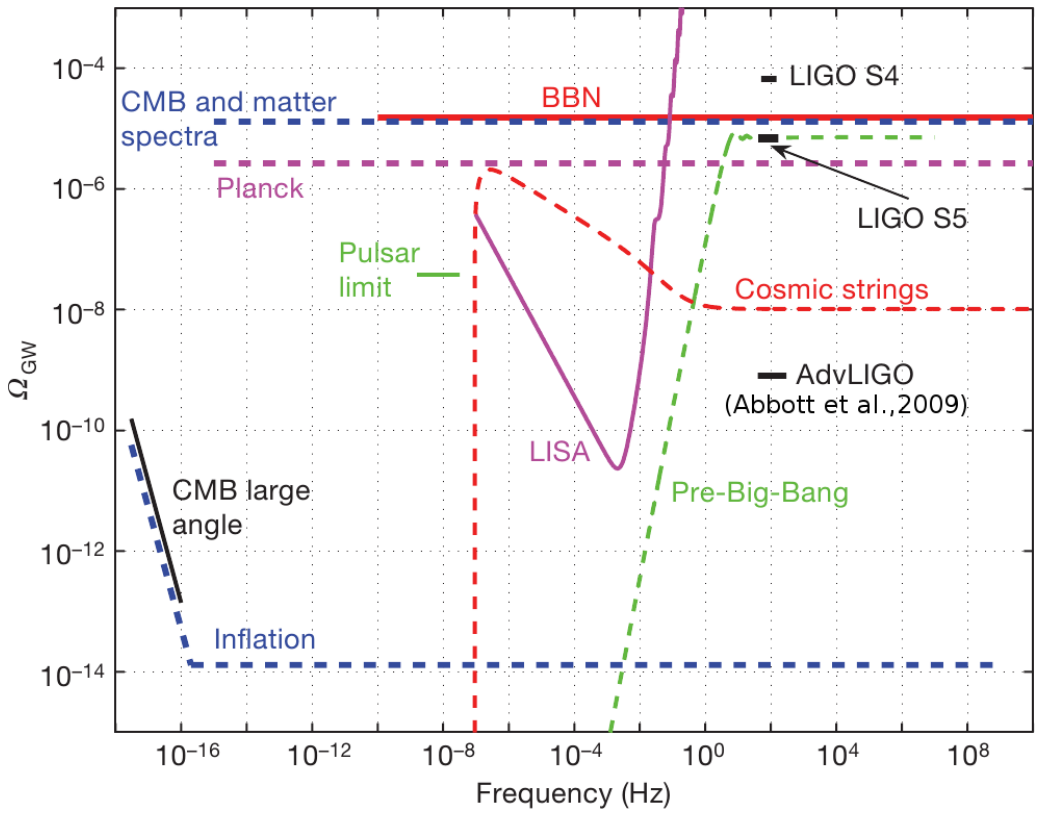

Figure 2: Comparison of the measurements for the SGWB energy density by means of the LIGO S4 and LIGO S5 data. Other indirect constrains are plotted: a constrain from the observed light nuclei abundance, produced by the Big Bang Nucleosynthesis (BBN), anisotropies in CMB at large angle, and the millisecond pulsar bound, based on the fluctuations in the pulse arrival times (adapted from B. P. Abbott et al.).

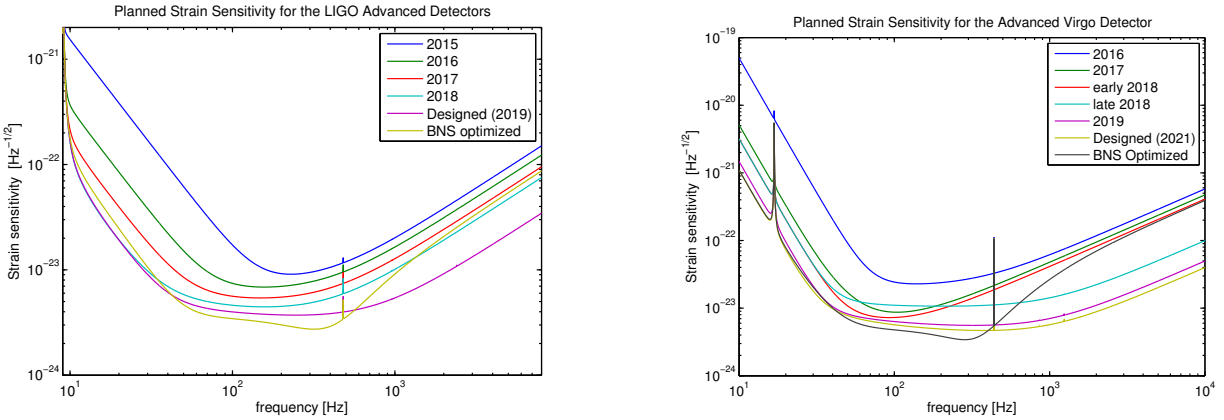

Figure 3: Data for the expected strain sensitivities at different stages of the upgrades are taken from [Aasi, 2013].

2 Cross-correlation analysis: a brief overview

We start with a brief summary of cross-correlation analysis, as derived in [Allen and Romano, 1999] and extended to include non-standard polarizations in [Nishizawa et al., 2009].

2.1 Cross-correlation including non-standard polarizations

To distinguish the SGWB signal $h(t)$ from stochastic detector noise $n(t)$, independent in each detector, one has to correlate signal between two detectors:

$$S \equiv \int_{-T/2}^{+T/2} \mathrm{d}t \int_{-T/2}^{+T/2} \mathrm{d}t'\, s_1(t) s_2(t')\, Q(t-t') \approx \int_{-\infty}^{+\infty} \mathrm{d}f \int_{-\infty}^{+\infty} \mathrm{d}f'\, \delta_T(f-f') \tilde{s}_1(t) \tilde{s}_2(t')\, \tilde{Q}(f') \quad (2)$$

Here $s_i(t)$ is the output of the i-th detector, which is supposed to be a linear superposition of GW strain signal and detector's intrinsic noise: $s_i(t) = h_i(t) + n_i(t)$. The function $Q(t-t')$ is a linear filter, which is chosen to optimize the SNR (to be defined yet). It depends on the separation orientation of the two detectors. The function $\delta_T(f)$ is defined as

$$\delta_T(f) \equiv \int_{-T/2}^{+T/2} \mathrm{d}t\, e^{-2\pi i f/t} = \frac{\sin(\pi f T)}{\pi f} \quad (3)$$

and it is weakly convergent to $\delta(f)$ for $T \to \infty$. T is the total observation time, $T \sim 10^7$ sec. Tilded quantities are Fourier transforms.

For a detector placed at a position $\mathbf{x}$, the SGWB strain signal $h(t, \mathbf{x})$ produced can be written as:

$$h(t,\mathbf{x}) = h_{ij}(t,\mathbf{x}) D^{ij} = \sum_{\substack{A=+,\times,x,\\ y,b,\ell}} \int_{S^2} \mathrm{d}^2\hat{\mathbf{\Omega}} \int_{-\infty}^{+\infty} \mathrm{d}f\, \tilde{h}^A\big(f,\hat{\mathbf{\Omega}}\big)\, e^{2\pi i\, f(t-\hat{\mathbf{\Omega}}\cdot\mathbf{x}/c)} F^A\big(\hat{\mathbf{\Omega}}\big) \quad (4)$$

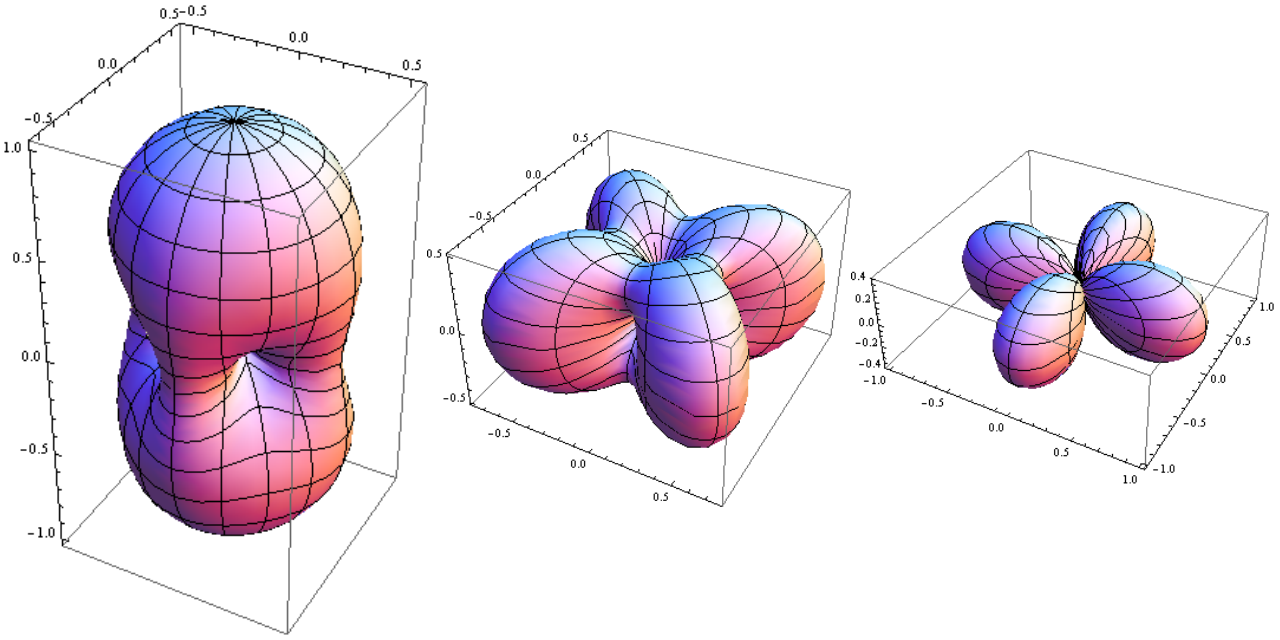

Figure 4: Angular pattern function for the tensor, vector and scalar modes, assuming no correlations between components. From left to right $F^T = \sqrt{(F^+)^2 + (F^\times)^2}$, $F^V = \sqrt{(F^x)^2 + (F^y)^2}$ and $F^S = \sqrt{(F^b)^2 + (F^\ell)^2}$ are represented.

where the gravitational metric perturbation $h_{ij}(t, \mathbf{x})$ is decomposed into the six polarization modes, $A = +, \times, x, y, b, \ell$, and analyzed by the Fourier transforms of their amplitudes $\tilde{h}^A(f, \hat{\mathbf{\Omega}})$. The quantity

$$F^A(\hat{\mathbf{\Omega}}) = D^{ij} e^A_{ij}(\hat{\mathbf{\Omega}})$$

which appears in Eq. (4) is the detector angular pattern function for the mode A, which is obtained by contracting the metric perturbation with the detector tensor D^{ij}. It gives a proportionality factor between the metric perturbation and the strain signal produced, for a given gravitational wave's propagation direction. As here we are interested in an isotropic background, we integrate in Eq. (4) over all the propagation directions $\hat{\mathbf{\Omega}}$.

Some examples of angular pattern functions are represented, as a polar diagram, in Figure 4.

The key point for extracting the GW strain from the cross-correlation S is taking its expectation value; in absence of intrinsic noise correlation between the two detectors, we have

$$\mu \equiv \langle S \rangle = \int_{-\infty}^{+\infty} \mathrm{d}f \int_{-\infty}^{+\infty} \mathrm{d}f' \, \delta_T(f - f') \langle \tilde{h}_1^*(f) \tilde{h}_2(f') \rangle \tilde{Q}(f'). \tag{5}$$

To evaluate the previous expectation value, we have to make some assumptions on the SGWB signal produced by any given theory [Allen and Romano, 1999, §II.B]. In the simplest model, which is the one we are interested to, we suppose the backgorund to be

Isotropic: this could be a first-order approximation, but we can expect it to hold from the comparison with the high isotropy of the CMBR;

Indipendently polarized *i.e.*, no correlation between different polarization modes;

Stationary, at least for the typical duration of a GW experiment, $T \sim 10^7$ sec, which is much smaller than the characteristic cosmological time scales;

a Gaussian random process, in this case the second-order moments $\langle h_i(t)h_j(t')\rangle$ completely specifies the statistical properties of the signal. This could be a very good first-order approximation, at least for cosmological backgrounds, granted by the central limit theorem.

Under these hypothesis we are allowed to write

$$\left\langle \tilde{h}^*_A(f,\hat{\mathbf{\Omega}})\tilde{h}_{A'}(f',\hat{\mathbf{\Omega}}')\right\rangle = \delta(f-f')\frac{\delta^2(\hat{\mathbf{\Omega}},\hat{\mathbf{\Omega}}')}{4\pi}\delta_{AA'}\frac{1}{2}S_h^A(|f|) \tag{6}$$

where $S_h^A(|f|)$ is the one-sided power spectral density of each polarization mode. These spectral densities fully characterize the stochastic background in our model.

It is more common to express the SGWB spectral density $S_h^A(|f|)$ in terms of the GWs energy density, per logarithmic frequency bin, normalized by the critical energy density of the Universe Nishizawa et al.:

$$\Omega^A_{\rm gw}(f) \equiv \frac{1}{\rho_c}\frac{{\rm d}\rho^A_{\rm gw}}{{\rm d}\ln f} = \left(\frac{2\pi^2}{3H_0^2}\right) f^3 S_h^A(f) \qquad A = +,\times,x,y,b,\ell. \tag{7}$$

Note that the above definition agrees with that of Nishizawa et al. but differs from that of Allen and Romano by a factor of two, since it is defined for each polarization mode.

It is convenient to represent the energy density in the form $h_0^2\Omega_{\rm gw}(f)$ by parameterizing the Hubble constant as $H_0 = 100\,h_0$ km s^{-1}Mpc^{-1}. In most of the cosmological scenarios, we assume that $+$ and $\times$ modes are not polarized, as well as the x and y modes. On the contrary, scalar modes could be correlated. Then

$$\Omega^T_{\rm gw} \equiv \Omega^+_{\rm gw} + \Omega^\times_{\rm gw}, \quad \left(\Omega^+_{\rm gw} = \Omega^\times_{\rm gw}\right) \tag{8}$$

$$\Omega^V_{\rm gw} \equiv \Omega^x_{\rm gw} + \Omega^y_{\rm gw}, \quad \left(\Omega^x_{\rm gw} = \Omega^y_{\rm gw}\right) \tag{9}$$

and

$$\Omega^S_{\rm gw} \equiv \Omega^b_{\rm gw} + \Omega^\ell_{\rm gw} = (1+\kappa)\Omega^b_{\rm gw} \tag{10}$$

where $\kappa = \Omega^\ell_{\rm gw}/\Omega^b_{\rm gw}$.

With the previous assumption, we can express the cross-correlation expectation value in terms of the SGWB energy density:

$$\begin{aligned}
\mu \equiv \langle S\rangle &\approx \iint_{-\infty}^{+\infty} {\rm d}f\,{\rm d}f'\;\delta_T(f-f')\left\langle \tilde{h}_1^*(f)\tilde{h}_2(f')\right\rangle \tilde{Q}(f') \\
&= \frac{3H_0^2}{4\pi^2}\int_{-\infty}^{+\infty}{\rm d}f|f|^{-3}\delta_T(0)\,\tilde{Q}(f)\sum_A \Omega^A_{\rm gw}(|f|)\int_{S^2}\frac{{\rm d}^2\hat{\mathbf{\Omega}}}{4\pi}\;F_1^A(\hat{\mathbf{\Omega}})F_2^A(\hat{\mathbf{\Omega}})e^{2\pi i f(\hat{\mathbf{\Omega}}\cdot\mathbf{x}_1 - \hat{\mathbf{\Omega}}\cdot\mathbf{x}_2)/c} \\
&\equiv \frac{3H_0^2}{20\pi^2}T\int_{-\infty}^{+\infty}{\rm d}f|f|^{-3}\tilde{Q}(f)\left[\Omega^T_{\rm gw}\gamma^T + \Omega^V_{\rm gw}\gamma^V + \xi\Omega^S_{\rm gw}\gamma^S\right]
\end{aligned} \tag{11}$$

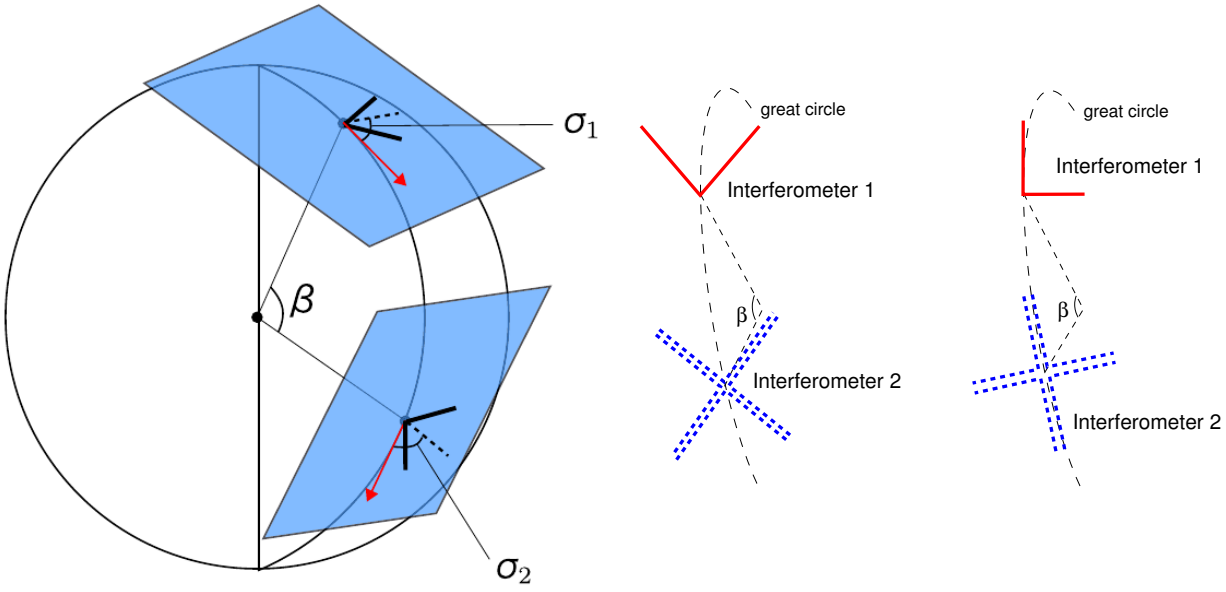

Figure 5: Coordinate system on the Earth for a detector pair. In the following we will distinguish between two particular orientations: the Type I (detectors' arms have the bisectors on the same plane, depicted in the middle) and the Type II (two arms of different detectors are on the same plane, depicted on the right).

where $\xi = (1+2\kappa)/6$. In the last line we have introduced the overlap reduction function (ORF), γ^M, for the polarization modes $M = T, V, S$:

$$\gamma^T(f) \equiv \frac{5}{2}\int_{S^2}\frac{\mathrm{d}^2\hat{\mathbf{\Omega}}}{4\pi}\left[F_1^+(\hat{\mathbf{\Omega}})F_2^+(\hat{\mathbf{\Omega}}) + F_1^\times(\hat{\mathbf{\Omega}})F_2^\times(\hat{\mathbf{\Omega}})\right]e^{2\pi i f\hat{\mathbf{\Omega}}\cdot\Delta\mathbf{x}/c} \tag{12}$$

$$\gamma^V(f) \equiv \frac{5}{2}\int_{S^2}\frac{\mathrm{d}^2\hat{\mathbf{\Omega}}}{4\pi}\left[F_1^x(\hat{\mathbf{\Omega}})F_2^x(\hat{\mathbf{\Omega}}) + F_1^y(\hat{\mathbf{\Omega}})F_2^y(\hat{\mathbf{\Omega}})\right]e^{2\pi i f\hat{\mathbf{\Omega}}\cdot\Delta\mathbf{x}/c} \tag{13}$$

$$\gamma^S(f) \equiv \frac{15}{1+2\kappa}\int_{S^2}\frac{\mathrm{d}^2\hat{\mathbf{\Omega}}}{4\pi}\left[F_1^b(\hat{\mathbf{\Omega}})F_2^b(\hat{\mathbf{\Omega}}) + \kappa F_1^\ell(\hat{\mathbf{\Omega}})F_2^\ell(\hat{\mathbf{\Omega}})\right]e^{2\pi i f\hat{\mathbf{\Omega}}\cdot\Delta\mathbf{x}/c} \tag{14}$$

The ORF represents how much degree of correlation between detectors in the GW signal is preserved. It takes into account the separation time delay between the two detectors and the non parallel alignment of the detector arms. ORF for several detector's pairs and modes are represented in Figure 6.

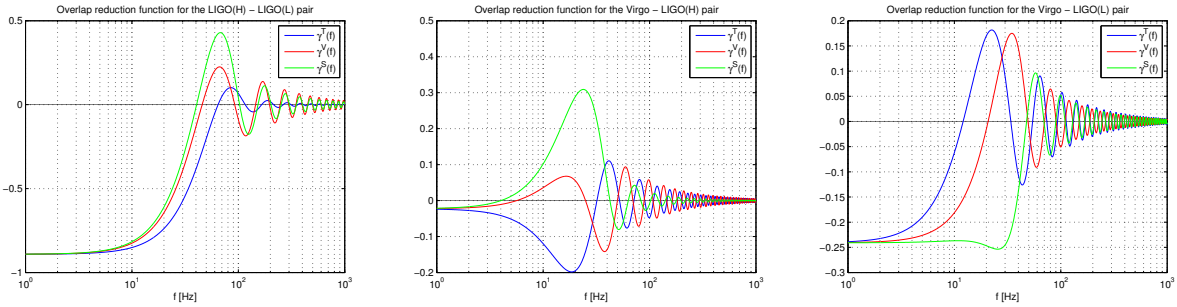

Figure 6: ORF for the different detector pairs Virgo - LIGO(L), Virgo - LIGO(H) and LIGO(H) - LIGO(L). Note how the difference of the behavior between the polarization modes appears at around the characteristic frequency $f_c \equiv c/2|\Delta \mathbf{x}|$, above of which the ORFs rapidly decrease to 0.

2.2 SNR for different polarizations

Assuming that the amplitude of the SGWB strain $h(t)$ is much smaller than the detector noise $n(t)$, we can calculate the variance of the cross-correlation signal:

$$\begin{aligned}\sigma^2 \equiv \langle S^2\rangle - \langle S\rangle^2 \approx \langle S^2\rangle &= \iint_{-\infty}^{+\infty} \mathrm{d}f\,\mathrm{d}f'\,\tilde{Q}(f)\tilde{Q}(f')\langle \tilde{s}_1^*(f)\tilde{s}_2(f)\tilde{s}_1^*(f')\tilde{s}_2(f')\rangle \\ &\approx \iint_{-\infty}^{+\infty} \mathrm{d}f\,\mathrm{d}f'\,\tilde{Q}(f)\tilde{Q}(f')\langle \tilde{n}_1^*(f)\tilde{n}_1(f')\rangle\langle \tilde{n}_2(f)\tilde{n}_2^*(f')\rangle \\ &\equiv \frac{T}{4}\int_{-\infty}^{+\infty} \mathrm{d}f\, P_1(|f|)P_2(|f|)|\tilde{Q}(f)| \end{aligned} \tag{15}$$

where we've introduced the one-sided power spectrum density of noise for the two detectors, $P_{1,2}(|f|)$. Introducing the signal-to-noise ratio

$$\mathrm{SNR} \equiv \frac{\mu}{\sqrt{\sigma^2}} \tag{16}$$

we can define the optimal filter function $\tilde{Q}(f)$ as the one which maximizes the SNR. Then, the optimal SNR can be written as [Nishizawa et al., 2009]:

$$\mathrm{SNR} = \frac{3H_0^2}{10\pi^2}\sqrt{T}\left[\int_{-\infty}^{+\infty} \mathrm{d}f\, \frac{\gamma^2(|f|)\Omega_{\mathrm{gw}}^2(|f|)}{f^6 P_1(|f|)P_2(|f|)}\right]^{1/2} \tag{17}$$

where $\gamma\Omega_{\mathrm{gw}} \equiv \gamma^T\Omega_{\mathrm{gw}}^T + \gamma^V\Omega_{\mathrm{gw}}^V + \gamma^S\Omega_{\mathrm{gw}}^S$.

Considering only one polarization mode at a time (setting $\Omega_{\mathrm{gw}}^M = 0$ for the others), we can compute the SNR for each mode. In the following we consider a flat stochastic background spectrum, $\Omega_{\mathrm{gw}} = cost.$

A normalized $SNR\,(\beta)$ is represented in Figure 7 for some relative orientations, as a function of β (see Figure 5 for the definition of β). The normalization is choosen in such a way that $\mathrm{SNR}(0) = 1$. Note that $SNR(0)$ is the same for all the polarizations, in the two orientations (Type I and ype II) considered. It is interesting to note how the SNR for the scalar mode is enhanced at relatively close detector distance. The same function is represented graphically in Figure 8, taking advanced Virgo as one of the two detectors.

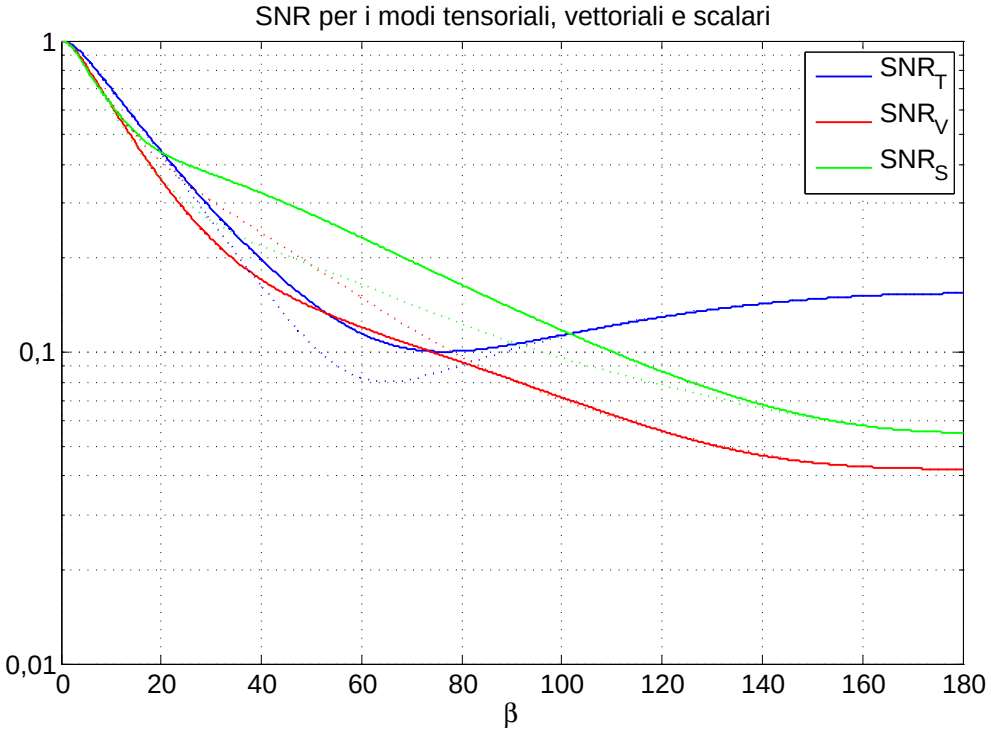

Figure 7: SNRs for different modes as a function of the separation angle β between the detectors. These functions are calculated for two different optimal configurations of the detectors' arms: solid lines are for Type I orientations and dashed lines are for Type II orientations (see Figure 5 for the definitions).

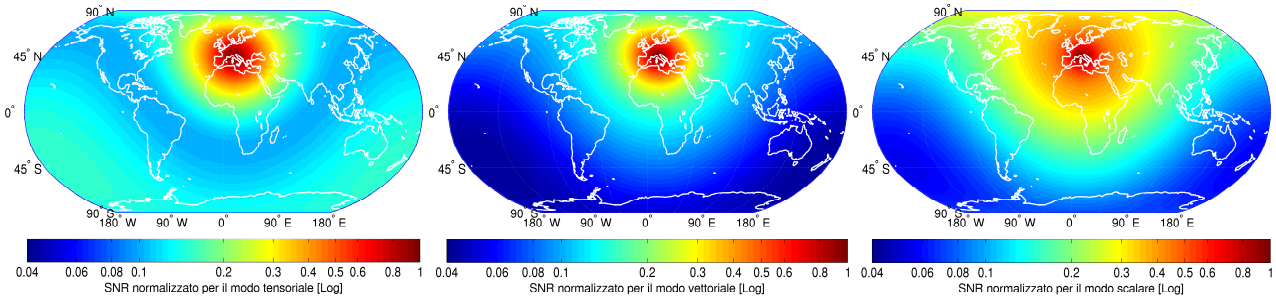

Figure 8: Color plot for the SNR for different modes of polarization. It is based on the Advanced Virgo detector with a possible partner placed somewhere allover the world. Strain sensitivity for the latter is taken equals to that of AdvLIGO. An optimal alignment of the arms is assumed.

2.3 Detection, statistical considerations: sensitivity level

Let us suppose that our experiments have gone on-line and are generating a certain amount of data. How can we decide, from the experimental data, if we've detected a SGWB? In particular,

- Assuming that a GW signal is present, how do we estimate its strength? and,
- what is the minimum value of $\Omega_{\rm gw}$ required to detect it, say, 95% of the time?

To answer these questions, some statistical considerations are needed [Allen and Romano, 1999]. We have to set up a statistical hypothesis test (from a frequentist point of view) and a decision rule that, given the outcome of an experiment, could allow us to answer the previous questions in a statistically rigorous way.

In the field of statistical signal analysis, this problem is worked out by means of the Neyman-Pearson Lemma (see [Allen and Romano, 1999, §IV.B] and [Kay, 1998, §6.4]).

Once we have the outcome of our cross-correlation experiment, we can calculate the estimators sample mean $\hat{\mu}$ and sample variance s^2 for the mean and the variance of the cross-correlation signal S. Then, the Neyman-Pearson Lemma tell us that: fixed a false alarm probability α, that is the maximum probability allowed for an erroneous detection, we can assert that a SGWB signal is present in our data if

$$\hat{\mu}\sqrt{n/s^2} \geqslant \sqrt{2}\,\mathrm{erfc}^{-1}(2\alpha) \tag{18}$$

with a detection probability

$$\gamma(\mu) = \frac{1}{2}\mathrm{erfc}\left(\mathrm{erfc}^{-1}(2\alpha) - \mu\sqrt{n/2\sigma^2}\right) \tag{19}$$

where $n \sim 10^4 \div 10^6$ is the number of samples of S we have extracted from the whole data stream. The dection probability defined by Eq. (19) is represented in Figure 6.

Assuming that a SGWB has been observed, we can answer to the remaining questions:

- we can estimate $\Omega_{\rm gw}$, by means of the value of μ, using the Neyman construction for confidence interval: in an ensemble of observation of the same SGWB, a fraction $1-\alpha$ of the intervals

$$I_\alpha \equiv \left[\hat{\mu} - \sqrt{2s^2/n}\,\mathrm{erfc}^{-1}(2\alpha), \hat{\mu} + \sqrt{2s^2/n}\,\mathrm{erfc}^{-1}(2\alpha)\right] \tag{20}$$

  constructed from the estimators $\hat{\mu}$ and s^2, will contain the value of the true mean μ.

- requiring that the detection rate be greater than a desired (fixed) rate γ, we can find the minimum detectable value of μ solving the inequality given by the Neyman-Pearson Lemma:

- For a power-law template for the SGWB energy density,

$$\Omega_{\rm gw}(f) = \Omega_\nu \left(\frac{f}{f_0}\right)^\nu \tag{21}$$

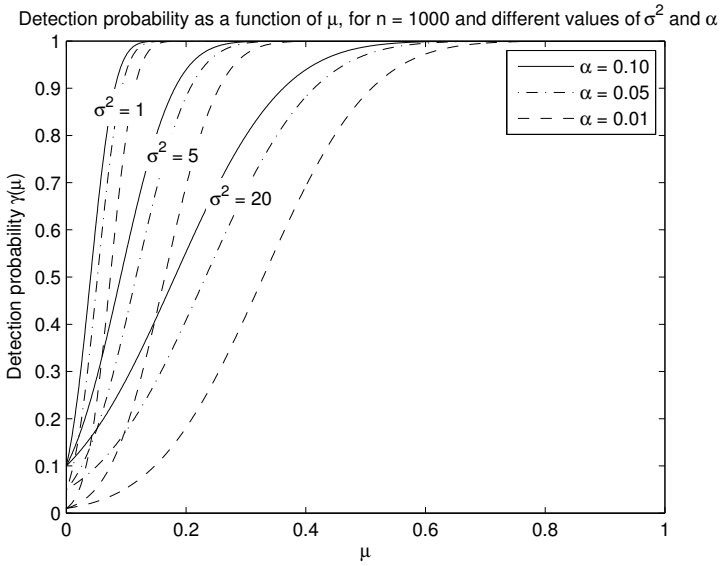

Figure 9: The detection probability $\gamma(\mu)$ as a function of μ, for several values of σ^2 and α.

where Ω_ν is a constant and f_0 a frequency of reference, as predicted by most theoretical models in the LIGO and Virgo frequency band, we can find the minimum SGWB detectable for each mode M:

$$\Omega_\nu^M \geqslant \frac{1}{\sqrt{T}} \frac{10\pi^2}{3H_0^2} \left[\int_{-\infty}^{+\infty} \mathrm{d}f \left(\frac{f}{f_0}\right)^{2\nu} \frac{\gamma_M^2(|f|)}{f^6 P_1(|f|) P_2(|f|)} \right]^{-1/2} \sqrt{2} \left(\mathrm{erfc}^{-1}(2\alpha) - \mathrm{erfc}^{-1}(2\gamma) \right) \tag{22}$$

depending on the noise power spectrum densities of the two detectors, $P_{1,2}(|f|)$, the duration of the experiment T, and on the false alarm and detection rates, α and γ.

3 Prospects on future results

Using the prospected power spectrum densities of the noise at the scheduled upgrades for the advanced detectors AdvLIGO and AdV, as reported in [Aasi, 2013], we can calculate the minimum values of the SGWB energy density detectable in near-future experiments.

Let us compute these values for a 4 months experiment ($T \simeq 10^7$ sec), for a false alarm rate $\alpha = 0.05$ and a detection rate $\gamma = 0.95$, and (in the case of power-law models for Ω_{gw}) for a reference frequency $f_0 = 100$ Hz.

3.1 SGWB sensitivity level

As a conclusion, we compare in Figure 14 the updated upper limits for different polarization modes with the current ones, using the values (for the flat case) taken from the previous tables.

It is interesting to observe that:

- sensitivity to scalar and vector modes is enhanced, with respect to the tensor mode, in the AdV - AdvLIGO detector pair, so it is possible to test these alternative polarizations;

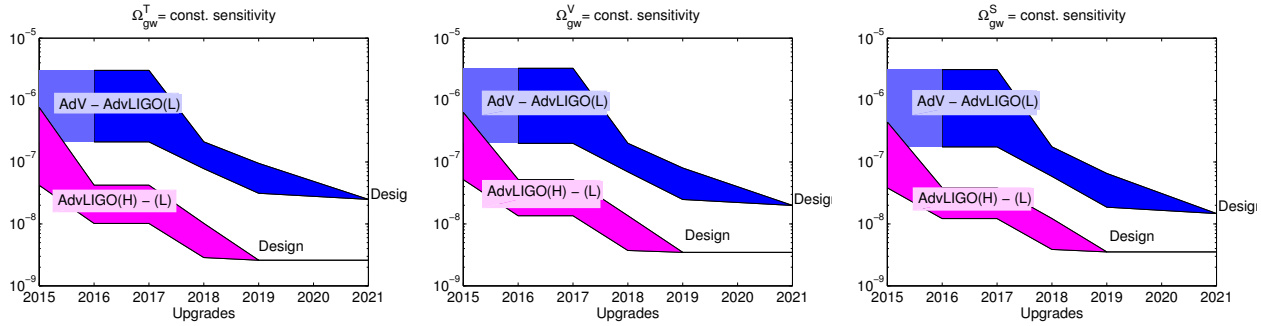

Mode	Detector pair	Early	Mid	Late	Designed
$h_0^2\,\Omega_0^T\big\vert_{95\%,5\%}$	AdV - AdvLIGO(L)	2.11×10^{-7}	7.82×10^{-8}	3.13×10^{-8}	2.49×10^{-8}
	AdvLIGO(L) - (H)	4.23×10^{-8}	1.02×10^{-8}	2.87×10^{-9}	2.59×10^{-9}
$h_0^2\,\Omega_0^V\big\vert_{95\%,5\%}$	AdV - AdvLIGO(L)	2.00×10^{-7}	6.94×10^{-8}	2.48×10^{-8}	1.99×10^{-8}
	AdvLIGO(L) - (H)	5.21×10^{-8}	1.35×10^{-8}	3.72×10^{-9}	3.47×10^{-9}
$\xi h_0^2\,\Omega_0^S\big\vert_{95\%,5\%}$	AdV - AdvLIGO(L)	1.75×10^{-7}	5.87×10^{-8}	1.86×10^{-8}	1.47×10^{-8}
	AdvLIGO(L) - (H)	3.83×10^{-8}	1.22×10^{-8}	3.87×10^{-9}	3.53×10^{-9}

Figure 10: Upper limits for a stochastic background spectrum $\Omega_{\rm gw}(f) = \Omega_0 = cost.$ The upper limit for the parameter Ω_0 is given as a function of the polarization, detector pair and epoch.

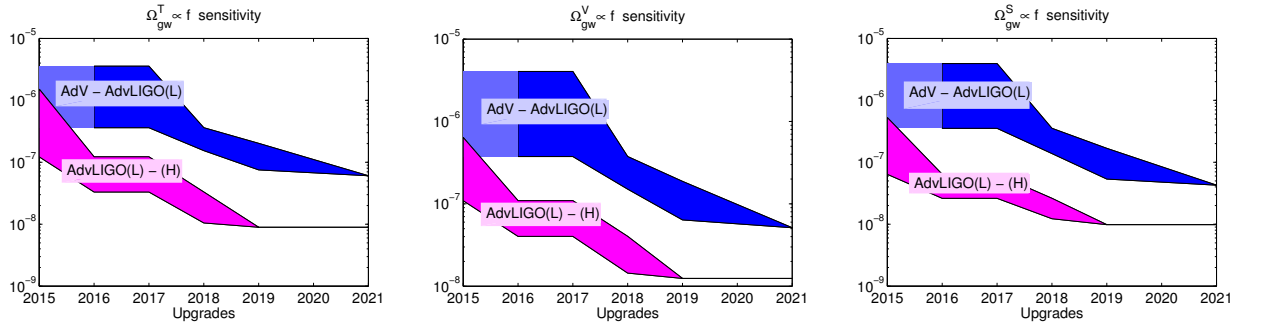

Mode	Detector pair	Early	Mid	Late	Designed
$h_0^2\,\Omega_1^T\big\vert_{95\%,5\%}$	AdV - AdvLIGO(L)	3.62×10^{-7}	1.54×10^{-7}	7.54×10^{-8}	6.06×10^{-8}
	AdvLIGO(L) - (H)	1.22×10^{-7}	3.31×10^{-8}	1.05×10^{-8}	8.92×10^{-9}
$h_0^2\,\Omega_1^V\big\vert_{95\%,5\%}$	AdV - AdvLIGO(L)	3.75×10^{-7}	1.54×10^{-7}	6.38×10^{-8}	5.13×10^{-8}
	AdvLIGO(L) - (H)	1.09×10^{-7}	4.03×10^{-8}	1.44×10^{-8}	1.24×10^{-8}
$\xi h_0^2\,\Omega_1^S\big\vert_{95\%,5\%}$	AdV - AdvLIGO(L)	3.53×10^{-7}	1.38×10^{-7}	5.36×10^{-8}	4.26×10^{-8}
	AdvLIGO(L) - (H)	6.40×10^{-8}	2.62×10^{-8}	1.23×10^{-8}	9.85×10^{-9}

Figure 11: Upper limits for a stochastic background spectrum $\Omega_{\rm gw}(f) = \Omega_1 \left(\frac{f}{100\ \rm Hz}\right)$. The upper limit for the parameter Ω_2 is given as a function of the polarization, detector pair and epoch.

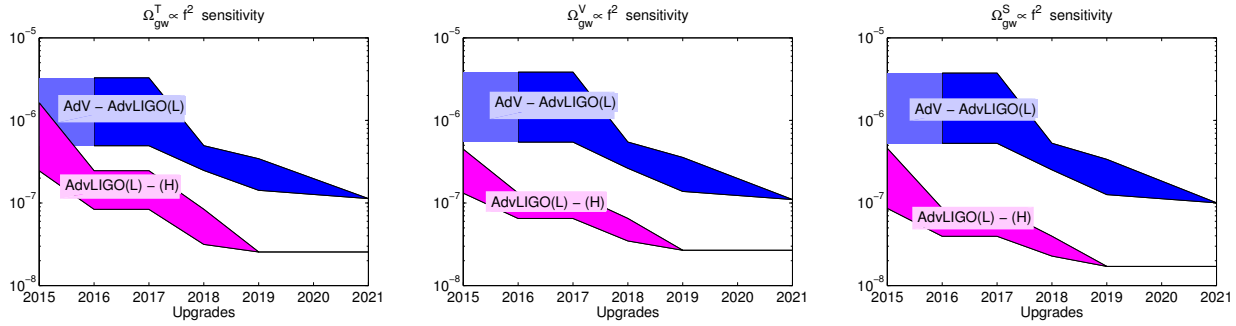

Mode	Detector pair	Early	Mid	Late	Designed
$h_0^2\,\Omega_2^T\big\vert_{95\%,5\%}$	AdV - AdvLIGO(L)	4.93×10^{-7}	2.48×10^{-7}	1.42×10^{-7}	1.13×10^{-7}
	AdvLIGO(L) - (H)	2.45×10^{-7}	8.39×10^{-8}	3.15×10^{-8}	2.55×10^{-8}
$h_0^2\,\Omega_2^V\big\vert_{95\%,5\%}$	AdV - AdvLIGO(L)	5.46×10^{-7}	2.64×10^{-7}	1.38×10^{-7}	1.10×10^{-7}
	AdvLIGO(L) - (H)	1.32×10^{-7}	6.50×10^{-8}	3.47×10^{-8}	2.68×10^{-8}
$\xi h_0^2\,\Omega_2^S\big\vert_{95\%,5\%}$	AdV - AdvLIGO(L)	5.28×10^{-7}	2.52×10^{-7}	1.26×10^{-7}	1.00×10^{-7}
	AdvLIGO(L) - (H)	8.61×10^{-8}	3.95×10^{-8}	2.28×10^{-8}	1.78×10^{-8}

Figure 12: Upper limits for a stochastic background spectrum $\Omega_{\rm gw}(f) = \Omega_2 \left(\frac{f}{100\ \rm Hz}\right)^2$. The upper limit for the parameter Ω_0 is given as a function of the polarization, detector pair and epoch.

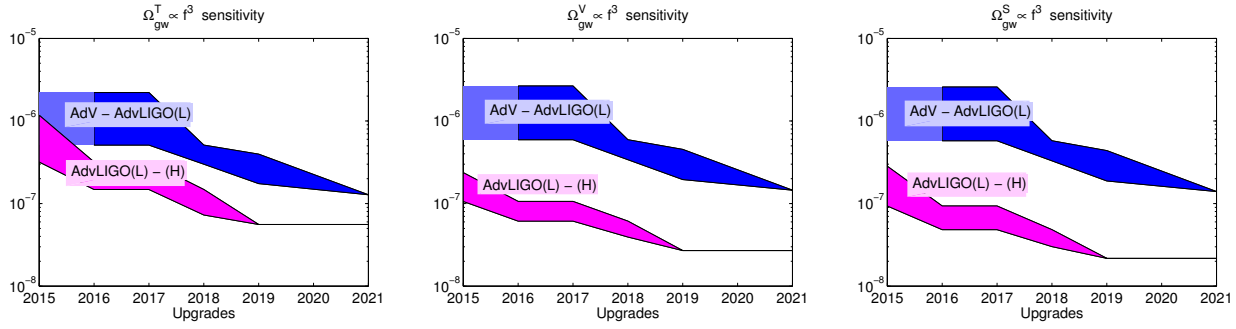

Mode	Detector pair	Early	Mid	Late	Designed
$h_0^2\,\Omega_3^T\big\vert_{95\%,5\%}$	AdV - AdvLIGO(L)	5.11×10^{-7}	3.00×10^{-7}	1.742×10^{-7}	1.27×10^{-7}
	AdvLIGO(L) - (H)	3.19×10^{-7}	1.48×10^{-7}	7.27×10^{-8}	5.58×10^{-8}
$h_0^2\,\Omega_3^V\big\vert_{95\%,5\%}$	AdV - AdvLIGO(L)	5.92×10^{-7}	3.40×10^{-7}	1.95×10^{-7}	1.45×10^{-7}
	AdvLIGO(L) - (H)	1.06×10^{-7}	6.12×10^{-8}	3.93×10^{-8}	2.69×10^{-8}
$\xi h_0^2\,\Omega_3^S\big\vert_{95\%,5\%}$	AdV - AdvLIGO(L)	5.76×10^{-7}	3.30×10^{-7}	1.87×10^{-7}	1.40×10^{-7}
	AdvLIGO(L) - (H)	9.33×10^{-8}	4.82×10^{-8}	3.01×10^{-8}	2.17×10^{-8}

Figure 13: Upper limits for a stochastic background spectrum $\Omega_{\rm gw}(f) = \Omega_3 \left(\frac{f}{100\ \rm Hz}\right)^3$. The upper limit for the parameter Ω_3 is given as a function of the polarization, detector pair and epoch.

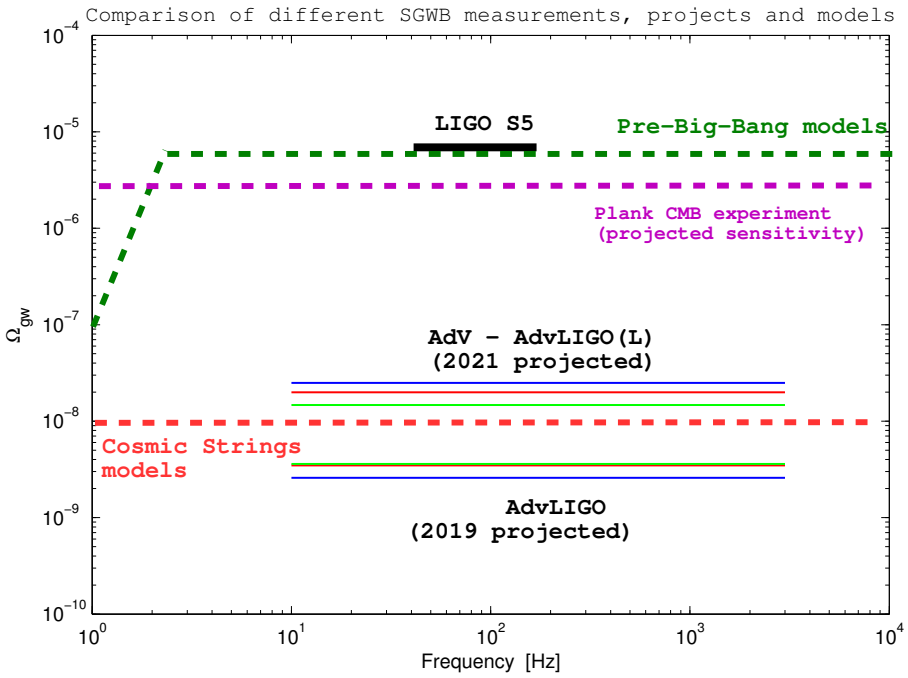

Figure 14: Comparison of different SGWB measurements, models and projected sensitivities for the advanced detectors AdV and AdvLIGO. Upper limits in the range of frequency of our interest are shown for tensor (blue), vector (red) and scalar (green) modes. Example of possible cosmic string (red dashed) and pre big bang model (green dashed) spectra are also shown (see [B. P. Abbott et al., 2009, Figure 2] for the references). Note that the amplitudes and spectral shapes of the shown models can vary significantly as a function of model parameters. On the right, the there is a detail of

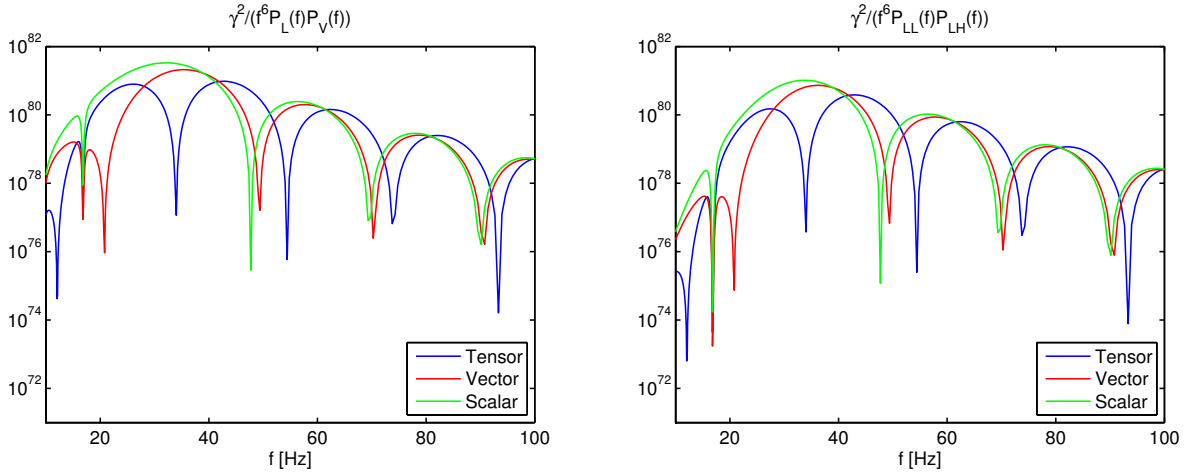

Figure 15: The integrand of the SNR formula (17), evaluated for the AdV-AdvLIGO pair (on the left) and for the AdvLIGO-AdvLIGO pair (on the right).

- on the contrary, with the AdvLIGO detectors, sensitivity to the tensor mode is enhanced, and is about one order of magnitude better than that achievable with the AdV - AdvLIGO pair;
- some models, like big bang models and cosmic strings models, predict densities that lie above the sensitivities predictable with the designed advanced detectors, so it could become at hand, in the near future ($\sim 2019 \div 2021$), testing these models.

3.2 Frequency contribution to the SNR

As regards the search for non-standard polarizations, it is interesting to focus on the integrand in the SNR formula (17).

It contains the contributions to the SNR due to the ORF and to the strain sensitivities of the two detectors. We plotted the results in Figure 15. Observing it at frequencies just before the critical frequency, $f_c = c/2|\Delta\mathbf{x}| \simeq 19 \div 51$, we can understand which polarization modes are most likely to be detectable; it turns out that the AdV-AdvLIGO detector pair is well suited to detect scalar polarization. Then, it could be used at a worth tool in the near-future GW astronomy for the study of alternative theories of gravity.

3.3 Modes separation

In discussing the detectability of the GW energy densities from non-standard polarization, $\Omega_{\rm gw}^M$, we just focussed on only one mode and set to 0 the energy density from the others. Actually, all these three modes are mixed in the detector cross-correlation signal.

The decomposition of the modes is an important issue and can be easily done generalizing the previous two detector cross-correlation analysis to the case of three (ore more) detectors [Nishizawa et al., 2009].

For the i-th and the j-th detector, we can define the statistic:

$$Z_{ij}(f) \equiv \frac{20\pi^2}{3H_0^2 T}|f|^3 \tilde{s}_i(f)\tilde{s}_j(f) \equiv \Omega_{\rm gw}^T(f)\gamma_{ij}^T(f) + \Omega_{\rm gw}^V\gamma_{ij}^V(f) + \Omega_{\rm gw}^S\gamma_{ij}^S(f) + \text{a noise term.} \quad (23)$$

Assuming once again uncorrelated noise between detector pairs, noise terms average to zero, and we get

$$\begin{pmatrix}\langle Z_{12}\rangle \\ \langle Z_{23}\rangle \\ \langle Z_{31}\rangle\end{pmatrix} = \mathbf{\Pi}\begin{pmatrix}\Omega_{\rm gw}^T \\ \Omega_{\rm gw}^V \\ \xi\Omega_{\rm gw}^S\end{pmatrix} \quad (24)$$

where

$$\mathbf{\Pi} \equiv \begin{pmatrix}\gamma_{12}^T & \gamma_{12}^V & \gamma_{12}^S \\ \gamma_{23}^T & \gamma_{23}^V & \gamma_{23}^S \\ \gamma_{31}^T & \gamma_{31}^V & \gamma_{31}^S\end{pmatrix} \quad (25)$$

is a detector correlation matrix. The polarization modes are separable as long as the detector correlation matrix $\mathbf{\Pi}$ is invertible, that is:

$$\det\mathbf{\Pi} = \gamma_{12}^T(\gamma_{23}^V\gamma_{31}^S - \gamma_{31}^V\gamma_{23}^S) + \gamma_{12}^V(\gamma_{23}^S\gamma_{31}^T - \gamma_{31}^S\gamma_{23}^T) + \gamma_{12}^S(\gamma_{23}^T\gamma_{31}^V - \gamma_{31}^T\gamma_{23}^V) \neq 0 \quad (26)$$

We can now derive the SNR formula for separate detection of each polarization mode with three detectors. From the inverse of the previous formula, one can find the cross-correlation average for the mode M as:

$$\mu_M = \frac{3H_0^2}{20\pi^2}T\int_{-\infty}^{+\infty} \mathrm{d}f\,|f|^{-3}\underbrace{\left[\eta_{M1}(f)\langle Z_{12}(f)\rangle + \eta_{M2}(f)\langle Z_{23}(f)\rangle + \eta_{M3}(f)\langle Z_{31}(f)\rangle\right]}_{H_g^M(f)}\tilde{Q}(f) \quad (27)$$

and a similar formula for the variance:

$$\sigma_M^2 = \frac{T}{4}\int_{-\infty}^{+\infty}\mathrm{d}f\underbrace{\left[\eta_{M1}^2(f)P_1(|f|)P_2(|f|) + \eta_{M2}^2(f)P_2(|f|)P_3(|f|) + \eta_{M3}^2(f)P_3(|f|)P_1(|f|)\right]}_{[H_n^M(f)]^2}|\tilde{Q}(f)|^2 \quad (28)$$

where η_{Mi}, for $M = T, V, S$ and $i = 1, 2, 3$, are the components of the inverse detector correlation matrix: $\eta_{Mi} \equiv (\mathbf{\Pi}^{-1})_{Mi}$. Then, optimizing their SNR one can find:

$$\mathrm{SNR}_M = \frac{3H_0^2}{10\pi^2}\sqrt{T}\left[\int_{-\infty}^{+\infty}\mathrm{d}f\frac{{H_g^M}^2(f)}{|f|^6{H_n^M}^2(f)}\right]^{1/2} \quad (29)$$

Using this formula one can calculate the exact sensitivity to each mode of polarization, in a three detector correlation analysis.

For simplicity, let us assume that all the three detectors have the same noise power spectrum $P(f)$. Then, the previous formula can be simplified in

$$\mathrm{SNR}_M = \frac{3H_0^2}{10\pi^2}\sqrt{T}\left[\int_{-\infty}^{+\infty}\mathrm{d}f\frac{{\Omega_{\rm gw}^M}^2(f)\,W^M(f)}{|f|^6P^2(f)}\right]^{1/2} \quad (30)$$

where

$$W^M(f) \equiv \left[\eta_{M1}^2 + \eta_{M2}^2 + \eta_{M3}^2\right]^{-1} \quad (31)$$

and $\sqrt{W^M(f)}$ can be interpreted as an effective overlap reduction function for the mode M in the case of three detector correlation mode separation. W_M is plotted as a function of the frequency in Figure 16.

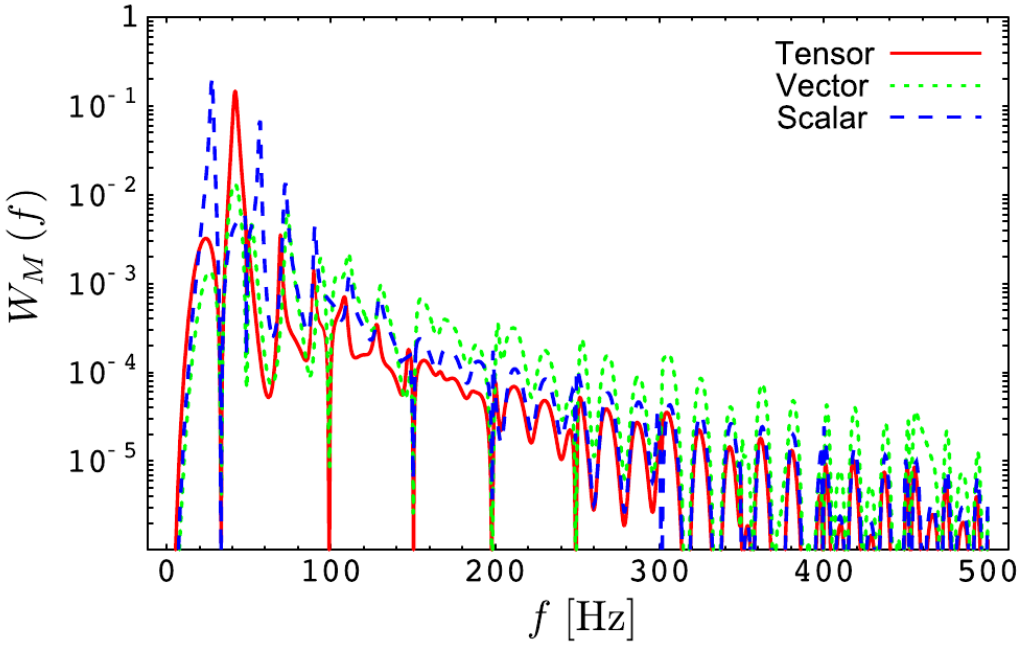

Figure 16: Plot of the squared effective overlap reduction function $W^M(f)$ for the AdV - AdvLIGO(H) - AdvLIGO(L) detector set. Picture adapted from [Nishizawa et al., 2009]. Here $h_0^2\Omega_{\rm gw}^T = 6.1 \times 10^{-9}$, $h_0^2\Omega_{\rm gw}^V = 1.3 \times 10^{-8}$ and $\xi h_0^2\Omega_{\rm gw}^S = 6.0 \times 10^{-9}$.

4 Conclusions

Most alternative theories of gravity have non-standard polarization modes. Tests of these polarizations, performed through the SGWB searches, is a valuable way of testing alternative theories of gravity. Cross-correlation analyses, using data from GW detectors, are appropriate for searching for additional polarization modes.

A network of three or more detectors can (in a model independent way) probe different polarizations and set constrains on theories beyond GR. We expect that it will possible to test or, at least, to pose some constrains on some cosmological and astrophysical models with the next generation advanced detectors.

The timeline of the sensitivities, achievable with the scheduled upgraded strain sensitivities for the advanced detectors AdV and AdvLIGO, outlines many previsions and possibilities for the near-future researches on cosmology and astrophysics, and, perhaps, on alternative theories of gravity.

References

Clifford Will. *Theory and experiment in gravitational physics*. Cambridge University Press, Cambridge England New York, NY, USA, 1993. ISBN 0521439736.

D.M. Eardley, D.L. Lee, A.P. Lightman, R.V. Wagoner, and C.M. Will. Gravitational-wave observations as a tool for testing relativistic gravity. *Phys.Rev.Lett.*, 30:884–886, 1973. doi: 10.1103/PhysRevLett.30.884.

Atsushi Nishizawa, Atsushi Taruya, Kazuhiro Hayama, Seiji Kawamura, and Masa-aki Sakagami. Probing nontensorial polarizations of stochastic gravitational-wave backgrounds with ground-based laser interferometers. *Phys. Rev. D*, 79:082002, Apr 2009. doi: 10.1103/PhysRevD.79.082002. URL `http://link.aps.org/doi/10.1103/PhysRevD.79.082002`.

B. B. P. Abbott, L. I. G. O. Scientific Collaboration & Virgo Collaboration, B. P. Abbott, R. Abbott, F. Acernese, R. Adhikari, P. Ajith, B. Allen, G. Allen, M. Alshourbagy, R. S. Amin, S. B. Anderson, W. G. Anderson, F. Antonucci, S. Aoudia, M. A. Arain, M. Araya, H. Armandula, P. Armor, K. G. Arun, Y. Aso, S. Aston, P. Astone, P. Aufmuth, C. Aulbert, S. Babak, P. Baker, G. Ballardin, S. Ballmer, C. Barker, D. Barker, F. Barone, B. Barr, P. Barriga, L. Barsotti, M. Barsuglia, M. A. Barton, I. Bartos, R. Bassiri, M. Bastarrika, Th S Bauer, B. Behnke, M. Beker, M. Benacquista, J. Betzwieser, P. T. Beyersdorf, S. Bigotta, I. A. Bilenko, G. Billingsley, S. Birindelli, R. Biswas, M. A. Bizouard, E. Black, J. K. Blackburn, L. Blackburn, D. Blair, B. Bland, C. Boccara, T. P. Bodiya, L. Bogue, F. Bondu, L. Bonelli, R. Bork, V. Boschi, S. Bose, L. Bosi, S. Braccini, C. Bradaschia, P. R. Brady, V. B. Braginsky, J. F J van den Brand, J. E. Brau, D. O. Bridges, A. Brillet, M. Brinkmann, V. Brisson, C. Van Den Broeck, A. F. Brooks, D. A. Brown, A. Brummit, G. Brunet, A. Bullington, H. J. Bulten, A. Buonanno, O. Burmeister, D. Buskulic, R. L. Byer, L. Cadonati, G. Cagnoli, E. Calloni, J. B. Camp, E. Campagna, J. Cannizzo, K. C. Cannon, B. Canuel, J. Cao, F. Carbognani, L. Cardenas, S. Caride, G. Castaldi, S. Caudill, M. CavagliÃ , F. Cavalier, R. Cavalieri, G. Cella, C. Cepeda, E. Cesarini, T. Chalermsongsak, E. Chalkley, P. Charlton, E. Chassande-Mottin, S. Chatterji, S. Chelkowski, Y. Chen, N. Christensen, C. T Y Chung, D. Clark, J. Clark, J. H. Clayton, F. Cleva, E. Coccia, T. Cokelaer, C. N. Colacino, J. Colas, A. Colla, M. Colombini, R. Conte, D. Cook, T. R C Corbitt, C. Corda, N. Cornish, A. Corsi, J-P. Coulon, D. Coward, D. C. Coyne, J. D E Creighton, T. D. Creighton, A. M. Cruise, R. M. Culter, A. Cumming, L. Cunningham, E. Cuoco, S. L. Danilishin, S. D'Antonio, K. Danzmann, A. Dari, V. Dattilo, B. Daudert, M. Davier, G. Davies, E. J. Daw, R. Day, R. De Rosa, D. Debra, J. Degallaix, M. Del Prete, V. Dergachev, S. Desai, R. Desalvo, S. Dhurandhar, L. Di Fiore, A. Di Lieto, M. Di Paolo Emilio, A. Di Virgilio, M. DÃaz, A. Dietz, F. Donovan, K. L. Dooley, E. E. Doomes, M. Drago, R. W P Drever, J. Dueck, I. Duke, J-C. Dumas, J. G. Dwyer, C. Echols, M. Edgar, A. Effler, P. Ehrens, G. Ely, E. Espinoza, T. Etzel, M. Evans, T. Evans, V. Fafone, S. Fairhurst, Y. Faltas, Y. Fan, D. Fazi, H. Fehrmann, I. Ferrante, F. Fidecaro, L. S. Finn, I. Fiori, R. Flaminio, K. Flasch, S. Foley, C. Forrest, N. Fotopoulos, J-D. Fournier, J. Franc, A. Franzen, S. Frasca, F. Frasconi, M. Frede, M. Frei, Z. Frei, A. Freise, R. Frey, T. Fricke, P. Fritschel, V. V. Frolov, M. Fyffe, V. Galdi, L. Gammaitoni, J. A. Garofoli, F. Garufi, E. Genin, A. Gennai, I. Gholami, J. A. Giaime, S. Giampanis, K. D. Giardina, A. Giazotto, K. Goda, E. Goetz, L. M. Goggin, G. GonzÃ¡lez, M. L. Gorodetsky, S. Gobler, R. Gouaty, M. Granata, V. Granata, A. Grant, S. Gras, C. Gray, M. Gray, R. J S Greenhalgh, A. M. Gretarsson, C. Greverie, F. Grimaldi, R. Grosso, H. Grote, S. Grunewald, M. Guenther, G. Guidi, E. K. Gustafson, R. Gustafson, B. Hage, J. M. Hallam, D. Hammer, G. D. Hammond, C. Hanna, J. Hanson, J. Harms, G. M. Harry, I. W. Harry, E. D. Harstad, K. Haughian, K. Hayama, J. Heefner, H. Heitmann, P. Hello, I. S. Heng, A. Heptonstall, M. Hewitson, S. Hild, E. Hirose, D. Hoak, K. A. Hodge, K. Holt, D. J. Hosken, J. Hough, D. Hoyland, D. Huet, B. Hughey, S. H. Huttner, D. R. Ingram, T. Isogai, M. Ito, A. Ivanov, B. Johnson, W. W. Johnson, D. I. Jones, G. Jones, R. Jones, L. Sancho de la Jordana, L. Ju, P. Kalmus, V. Kalogera, S. Kandhasamy, J. Kanner, D. Kasprzyk, E. Katsavounidis, K. Kawabe, S. Kawamura, F. Kawazoe, W. Kells, D. G. Keppel, A. Khalaidovski, F. Y. Khalili, R. Khan, E. Khazanov, P. King, J. S. Kissel, S. Klimenko, K. Kokeyama, V. Kondrashov, R. Kopparapu, S. Koranda, D. Kozak, B. Krishnan, R. Kumar, P. Kwee, P. La Penna, P. K. Lam, M. Landry, B. Lantz, M. Laval, A. Lazzarini, H. Lei, M. Lei, N. Leindecker, I. Leonor, N. Leroy, N. Letendre, C. Li, H. Lin, P. E. Lindquist, T. B. Littenberg, N. A. Lockerbie, D. Lodhia, M. Longo, M. Lorenzini, V. Loriette, M. Lormand, G. Losurdo, P. Lu, M. Lubinski, A. Lucianetti, H. LÃŒck, B. Machenschalk, M. Macinnis, J-M. Mackowski, M. Mageswaran, K. Mailand, E. Majorana, N. Man, I. Mandel, V. Mandic, M. Mantovani, F. Marchesoni, F. Marion, S. MÃ¡rka, Z. MÃ¡rka, A. Markosyan, J. Markowitz, E. Maros, J. Marque, F. Martelli, I. W. Martin, R. M. Martin, J. N. Marx, K. Mason, A. Masserot, F. Matichard, L. Matone, R. A. Matzner, N. Mavalvala, R. McCarthy, D. E. McClelland, S. C. McGuire, M. McHugh, G. McIntyre, D. J A McKechan, K. McKenzie, M. Mehmet, A. Melatos, A. C. Melissinos, G. Mendell, D. F. MenÃ©ndez, F. Menzinger, R. A. Mercer, S. Meshkov, C. Messenger, M. S. Meyer, C. Michel, L. Milano, J. Miller, J. Minelli, Y. Minenkov, Y. Mino, V. P. Mitrofanov, G. Mitselmakher, R. Mittleman, O. Miyakawa, B. Moe, M. Moh. An upper limit on the stochastic gravitational-wave background of cosmological origin. *Nature*, 460(7258):990–994, Aug 2009. doi: 10.1038/nature08278. URL `http://dx.doi.org/10.1038/nature08278`.

J. et al. Aasi. Prospects for localization of gravitational wave transients by the advanced ligo and advanced virgo observatories. 2013.

B Allen and J D Romano. Detecting a stochastic background of gravitational radiation: Signal processing strategies and sensitivities. *Phys. Rev. D*, 59(gr-qc/9710117. WISC-MILW-97-TH-14. 10):102001, 1999.

S.M. Kay. *Fundamentals of Statistical Signal Processing: Detection theory*. Prentice Hall Signal Processing Series. Prentice-Hall PTR, 1998. ISBN 9780135041352. URL `http://books.google.it/books?id=vA9LAQAAIAAJ`.